# Dual and Joint EKF for Simultaneous SOC and SOH Estimation

Gregory L. Plett

## Abstract

A battery management system for HEV/BEV application must perform a number of estimation tasks in real time. In previous papers, we have presented methods for cell SOC estimation that use extended Kalman filters (EKF) as their basis. In this paper, we show how EKF may also be used to estimate power fade, capacity fade, and can keep the SOC estimate accurate throughout the lifetime of the cell, even though its dynamics change as it ages. Results are presented to demonstrate the efficacy of the new methods. 

**Keywords:** Algorithmic, calculation, state of charge, lithium polymer, HEV.

## 1. Introduction

A battery management system for HEV and other applications must perform a number of estimation tasks in real time. In previous papers [1–6], we have presented methods for cell SOC estimation that use extended Kalman filters (EKF) as their basis. EKF requires a precise model of cell dynamics and repeatedly performs three steps. It uses the model to (1) predict cell terminal voltage based on its best estimate of the cell's state and available measurements. This prediction is (2) compared to measured cell voltage. Any difference between the prediction and measurement may be attributed to either measurement error (*e.g.*, sensor noise), modeling error, or an error in the state estimate. The EKF (3) carefully updates the model state, using the prediction error and a weighting function that takes into account that state-error is not the only source of prediction error.

For EKF to give peak performance, the cell model being used must predict true cell behavior as exactly as possible. However, cells are not created equal, even in mass production, so a single model will not give peak performance in a pack comprising many cells. A further complication is that cell dynamics (especially their resistance and total capacity) change as the cells age, both in calendar life and accumulated cycles, and that cells do not all age at the same rate.

Ideally, we would like separate models for each cell, where each is initialized with a nominal version of new-cell dynamics and adapts over time to more accurately capture the present cell dynamics. An added benefit of an adaptive cell model is that parameters indicative of the level of cell deterioration, such as present resistance and present total capacity, are worth estimating in their own right, as they are useful in composing estimates of cell state-of-health (SOH).

This paper describes methods within the framework of EKF that simultaneously estimate the state (including SOC) and parameters (including resistance and total capacity) of a cell model. We first review the EKF method, and then show how it may be extended to estimate both state and parameters. To apply to the battery-management-system application, we then review a mathematical cell model that may be used. Since the proposed methods are computationally intensive, they may not be feasible for every application; so simplified versions are given for monitoring capacity fade and power fade. Results are presented and conclusions made.

## 2. Review of EKF

The Kalman filter is the optimum state estimator for a linear system under certain assumptions. If the system is nonlinear, then we may use a linearization process at every time step to approximate the

nonlinear system with a linear time-varying (LTV) system. This LTV system is then used in the Kalman filter, resulting in an extended Kalman filter (EKF) on the true nonlinear system. Note that although EKF is not necessarily optimal, it often works very well.

To use an EKF to estimate a system's state, we must have a "state-space" model of its dynamics:

$$x_{k+1} = f(x_k, u_k) + w_k \quad (1)$$

$$y_k = g(x_k, u_k) + v_k, \quad (2)$$

where, $w_k$ and $v_k$ are zero mean white Gaussian stochastic processes with covariance matrices $\Sigma_w$ and $\Sigma_v$, respectively, and model state noise and sensor noise. In (1), $f(\ )$ is a nonlinear transition matrix function and in (2), $g(\ )$ is a nonlinear measurement matrix function.

The EKF, based on these equations, is a recursive algorithm to update an estimate $\hat{x}_k$ of the present state $x_k$. It repeatedly performs a sequence of steps. First, it predicts the present state given the past state estimate and the system input. Then it predicts the uncertainty of the state estimate $\Sigma_{\tilde{x},k}$. A measurement of the system output is made and compared with a prediction of the output based on the state estimate. The state estimate is updated based on the prediction error, the sensitivity of the output to various states, and the uncertainty of the states. The state-estimate uncertainty is also updated. The algorithm is summarized in Table 1, and is described in more detail in references [2–6]. The notation uses a superscript "–" to denote a predicted quantity, a superscript "+" to denote an updated quantity, a circumflex "^" to dentote an estimated quantity, a tilde "~" to denote an estimation error, and $\Sigma$ to denote the covariance of an estimated quantity.

# 3. Joint and Dual EKF Methods

The system state $x_k$ includes, at least, a minimum amount of information, together with the present input and a mathematical model of the cell, needed to predict the present output. The state might include: SOC, polarization voltage levels with respect to different time constants, and hysteresis levels, for example. Members of the system state vector have the ability to change rapidly with respect to time, such as SOC, which might traverse its entire range in a few minutes. The system parameters $\theta_k$ are the values that change only slowly with time, in such a way that they may not be directly determined with knowledge of the system measured input and output. These might include: cell capacity (possibly different values for charge/discharge), resistance(s), polarization voltage time constant(s), polarization voltage blending factor(s), hysteresis blending factor(s), hysteresis rate constant(s), efficiency factor(s), and so forth. Generally, we would like to be able to estimate both the cell state and the cell parameters.

There are two basic approaches to generalizing EKF to simultaneously estimate both state and parameters. Joint estimation augments the state vector of the system with the parameters, and uses an extended Kalman filter on the augmented system with large matrix operations. Dual estimation uses two cooperating extended Kalman filters where one estimates the state and the other estimates the parameters. These two methods are described in the following sections.

## 3.1. Joint EKF

We begin our discussion of joint EKF by defining a model for the dynamics of cell parameters:

$$\theta_{k+1} = \theta_k + r_k. \quad (3)$$

The equation states that the parameters are essentially constant, but that they may change slowly over time, modeled by a fictitious "noise" process denoted, $r_k$.

Within a joint filter, the dynamics of the state and the dynamics of the parameters are combined to make an augmented system:

$$\begin{bmatrix} x_{k+1} \\ \theta_{k+1} \end{bmatrix} = \begin{bmatrix} f(x_k, u_k, \theta_k) \\ \theta_k \end{bmatrix} + \begin{bmatrix} w_k \\ r_k \end{bmatrix}$$
$$y_k = g(x_k, u_k, \theta_k) + v_k.$$

Note that to simplify notation, we will refer to the vector comprising the present state and present parameters as $\chi_k$, and the equation combining the dynamics of the state and the dynamics of the parameters as $\mathcal{F}$. This allows us to write

$$\chi_{k+1} = \mathcal{F}(\chi_k, u_k) + \begin{bmatrix} w_k \\ r_k \end{bmatrix}$$
$$y_k = g(\chi_k, u_k) + v_k.$$

With the augmented model of the system state dynamics and parameter dynamics defined, we apply the EKF method. Table 2 gives a listing of the steps. The procedure is initialized by setting the augmented state estimate $\hat{\chi}_0$ to the best guess of the true augmented state by setting the top portion to $E[x_0]$ and the bottom portion to $E[\theta_0]$. The estimation-error covariance matrix $\Sigma_{\tilde{\chi}}^{+}$ is also initialized. The rest of the steps are similar to the standard EKF, but with larger matrix operations.

### 3.2. Dual EKF

With dual EKF, separate filters are used to estimate the state and parameters. The parameter filter uses a model of dynamics from Equation (3) and the cell model output equation giving:

$$\begin{aligned} \theta_{k+1} &= \theta_k + r_k \\ d_k &= g(x_k, u_k, \theta_k) + e_k. \end{aligned} \tag{4}$$

Again, the first equation states that the parameters are essentially constant, but that they may change slowly over time, modeled by a fictitious "noise" process denoted, $r_k$. The "output" of the optimum parameter dynamics is the cell output estimate plus some estimation error $e_k$.

With models of the system state dynamics and parameter dynamics defined, dual extended Kalman filters are employed. Table 3 is a listing of the full algorithm. The procedure is initialized by setting the parameter estimate $\hat{\theta}$ to the best guess of the true parameters, and by setting the state estimate $\hat{x}$ to the best estimate of the cell state. The estimation-error covariance matrices $\Sigma_{\tilde{x}}^{+}$ and $\Sigma_{\tilde{\theta}}^{+}$ are also initialized. For example, an initialization of SOC might be estimated/based on a cell voltage in a look-up table, or information that was previously stored when a battery pack/cell was last powered down. Other examples might incorporate the length of time that the battery system had rested since power-down and the like. The remainder of the algorithm steps compute the two extended Kalman filters, with appropriate information interchange. A block diagram of the method is shown in Figure 1.

The only subtle point is the calculation of $C_k^{\theta}$, which requires a total-differential expansion to be correct. To compute $C_k^{\theta}$,

$$\frac{d\, g(\hat{x}_k^-, u_k, \theta_k)}{d\,\theta} = \frac{\partial\, g(\hat{x}_k^-, u_k, \theta_k)}{\partial\,\theta} + \frac{\partial\, g(\hat{x}_k^-, u_k, \theta_k)}{\partial\, \hat{x}_k^-} \frac{d\, \hat{x}_k^-}{d\,\theta}$$

$$\frac{d\, \hat{x}_k^-}{d\,\theta} = \frac{\partial\, f(\hat{x}_{k-1}^+, u_{k-1}, \theta_k^-)}{\partial\,\theta} + \frac{\partial\, f(\hat{x}_{k-1}^+, u_{k-1}, \theta_k^-)}{\partial\, \hat{x}_{k-1}^+} \frac{d\, \hat{x}_{k-1}^+}{d\,\theta}$$

$$\frac{d\, \hat{x}_{k-1}^+}{d\,\theta} = \frac{d\, \hat{x}_{k-1}^-}{d\,\theta} - L_k^x \frac{d\, g(\hat{x}_{k-1}^-, u_{k-1}, \theta_{k-1})}{d\,\theta},$$

assuming that $L_k^x$ is not a function of $\theta$ (it is—weakly—so that it is not worth the extra computation to include effects of $L_k^x$ as a function of $\theta$). The three total derivatives are computed recursively, with the result stored each iteration. The partials are computed each time step.

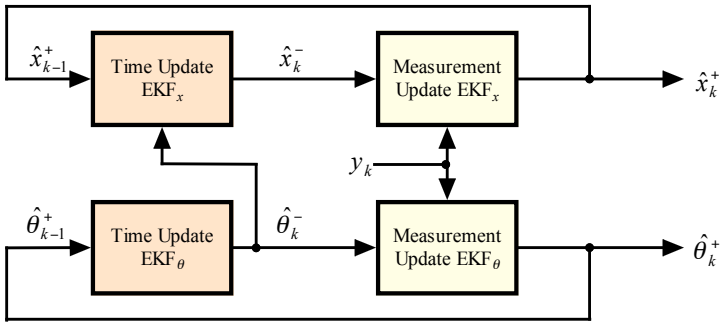


**Figure 1:** Block diagram of dual extended Kalman filtering.

### 3.3 Convergence

The dual/joint extended Kalman filters will adapt $\hat{x}$ and $\hat{\theta}$ so that the model input-output relationship matches the cell input-output data as closely as possible. There is no built-in guarantee that the state or parameters of the model converge to anything with physical meaning. We take special steps to ensure that this occurs.

A very crude cell model may be used, combined with the dual/joint EKF, to ensure convergence of the SOC state. Specifically,

$$y_k \approx \mathrm{OCV}(z_k) - Ri_k$$
$$\mathrm{OCV}(z_k) \approx y_k + Ri_k$$
$$\hat{z}_k = \mathrm{OCV}^{-1}(v_k + Ri_k).$$

By measuring the cell voltage under load, the cell current, and having knowledge of $R$, (perhaps through $\hat{\theta}$ from the dual/joint EKF), and knowing the inverse OCV function for the cell chemistry, one can compute a noisy estimate of SOC, $\hat{z}_k$.

To combine this simple model with the dual/joint EKF, the cell model being used for dual estimation (*e.g.*, perhaps the ESC model) has its output equation augmented with SOC:

$$g(x_k, u_k, \theta) = \begin{bmatrix} \mathrm{OCV}(z_k) - Ri_k + h_k + Gf_k \\ z_k \end{bmatrix}.$$

The dual EKF is run on this modified model, with the "measured" information in the measurement update being

$$\begin{bmatrix} v_k \\ \hat{z}_k \end{bmatrix}.$$

While the "noise" of $\hat{z}_k$ (short-term bias due to hysteresis effects and polarization filter voltages being ignored) prohibit it from being used as the primary estimator of SOC, its expected long-term behavior in a dynamic environment is accurate, and maintains the accuracy of the SOC state in the dual EKF.

**Table 1:** Summary of the extended Kalman filter, adapted from reference [10].

*State-space model:*

$$x_{k+1} = f(x_k, u_k) + w_k$$
$$y_k = g(x_k, u_k) + v_k \quad ,$$

where $w_k$ and $v_k$ are independent, zero-mean, Gaussian noise processes of covariance matrices $\Sigma_w$ and $\Sigma_v$, respectively.

*Definitions:* $A_k = \left.\frac{\partial f(x_k, u_k)}{\partial x}\right|_{x_k = \hat{x}_k^+}$ $\qquad C_k = \left.\frac{\partial g(x_k, u_k)}{\partial x}\right|_{x_k = \hat{x}_k^-}$

*Initialization:* For $k = 0$, set $\hat{x}_0^+ = E[x_0]$, $\Sigma_{\tilde{x},0}^+ = E[(x_0 - E[x_0])(x_0 - E[x_0])^T]$.

*Computation:* For $k = 1,2,\ldots$, compute:

Time update:
$$\hat{x}_k^- = f(\hat{x}_{k-1}^+, u_{k-1}).$$
$$\Sigma_{\tilde{x},k}^- = A_{k-1}\Sigma_{\tilde{x},k-1}^+ A_{k-1}^T + \Sigma_w.$$

Measurement update:
$$L_k = \Sigma_{\tilde{x},k}^- C_k^T [C_k \Sigma_{\tilde{x},k}^- C_k^T + \Sigma_v]^{-1}.$$
$$\hat{x}_k^+ = \hat{x}_k^- + L_k[y_k - g(\hat{x}_k^-, u_k)].$$
$$\Sigma_{\tilde{x},k}^+ = (I - L_k C_k)\Sigma_{\tilde{x},k}^-.$$

**Table 2:** Joint extended Kalman filter for state and weight update, adapted from [10].

*State-space models:*

$$\begin{bmatrix} x_{k+1} \\ \theta_{k+1} \end{bmatrix} = \begin{bmatrix} f(x_k, u_k, \theta_k) \\ \theta_k \end{bmatrix} + \begin{bmatrix} w_k \\ r_k \end{bmatrix} \quad \text{or} \quad \chi_{k+1} = \mathcal{F}(\chi_k, u_k) + \begin{bmatrix} w_k \\ r_k \end{bmatrix}$$
$$y_k = g(x_k, u_k, \theta_k) + v_k. \qquad y_k = g(\chi_k, u_k) + v_k.$$

where $w_k$, $v_k$, and $r_k$ are independent, zero-mean, Gaussian noise processes of covariance matrices $\Sigma_w$, $\Sigma_v$, and $\Sigma_r$, respectively.

*Definitions:* $A_{k-1} = \left.\frac{\partial \mathcal{F}(\chi_{k-1}, u_{k-1})}{\partial \chi_{k-1}}\right|_{\chi_{k-1} = \hat{\chi}_{k-1}^+}$ $\qquad C_k = \left.\frac{\partial g(\chi_k, u_k)}{\partial \chi_k}\right|_{\chi_k = \hat{\chi}_k^-}$

*Initialization:* For $k = 0$, set $\hat{\chi}_0^+ = E[\chi_0]$, $\quad \Sigma_{\tilde{\chi},0}^+ = E[(\chi_0 - \hat{\chi}_0^+)(\chi_0 - \hat{\chi}_0^+)^T]$.

*Computation:* For $k = 1,2,\ldots,$ compute:

Time update:
$$\hat{\chi}_k^- = \mathcal{F}(\hat{\chi}_{k-1}^+, u_{k-1})$$
$$\Sigma_{\tilde{\chi},k}^- = A_{k-1}\Sigma_{\tilde{\chi},k-1}^+ A_{k-1}^T + \text{diag}(\Sigma_w, \Sigma_r).$$

Measurement update:
$$L_k = \Sigma_{\tilde{\chi},k}^- (C_k)^T [C_k \Sigma_{\tilde{\chi},k}^- (C_k)^T + \Sigma_v]^{-1}$$
$$\hat{\chi}_k^+ = \hat{\chi}_k^- + L_k[y_k - g(\hat{\chi}_k^-, u_k)]$$
$$\Sigma_{\tilde{\chi},k}^+ = (I - L_k C_k)\Sigma_{\tilde{\chi},k}^-.$$

**Table 3:** Dual extended Kalman filter for state and weight update, adapted from [10].

*State-space models:*

$$\begin{aligned} x_{k+1} &= f(x_k, u_k, \theta_k) + w_k \\ y_k &= g(x_k, u_k, \theta_k) + v_k \end{aligned} \quad \text{and} \quad \begin{aligned} \theta_{k+1} &= \theta_k + r_k \\ d_k &= g(x_k, u_k, \theta_k) + e_k, \end{aligned}$$

where $w_k$, $v_k$, $r_k$ and $e_k$ are independent, zero-mean, Gaussian noise processes of covariance matrices $\Sigma_w$, $\Sigma_v$, $\Sigma_r$ and $\Sigma_e$, respectively.

*Definitions:*

$$A_{k-1} = \left.\frac{\partial f(x_{k-1}, u_{k-1}, \hat{\theta}_k^-)}{\partial x_{k-1}}\right|_{x_{k-1}=\hat{x}_{k-1}^+} \qquad C_k^x = \left.\frac{\partial g(x_k, u_k, \hat{\theta}_k^-)}{\partial x_k}\right|_{x_k=\hat{x}_k^-} \qquad C_k^\theta = \left.\frac{d\, g(\hat{x}_k^-, u_k, \theta)}{d\,\theta}\right|_{\theta=\hat{\theta}_k^-}$$

*Initialization:* For $k = 0$, set

$$\begin{aligned} \hat{\theta}_0^+ &= E[\theta_0], \quad \Sigma_{\tilde{\theta},0}^+ = E[(\theta_0 - \hat{\theta}_0^+)(\theta_0 - \hat{\theta}_0^+)^T] \\ \hat{x}_0^+ &= E[x_0], \quad \Sigma_{\tilde{x},0}^+ = E[(x_0 - \hat{x}_0^+)(x_0 - \hat{x}_0^+)^T]. \end{aligned}$$

*Computation:* For $k = 1,2,\ldots,$ compute:

Time update for the weight filter

$$\begin{aligned} \hat{\theta}_k^- &= \hat{\theta}_{k-1}^+ \\ \Sigma_{\tilde{\theta},k}^- &= \Sigma_{\tilde{\theta},k-1}^+ + \Sigma_r. \end{aligned}$$

Time update for the state filter

$$\begin{aligned} \hat{x}_k^- &= f(\hat{x}_{k-1}^+, u_{k-1}, \hat{\theta}_k^-) \\ \Sigma_{\tilde{x},k}^- &= A_{k-1}\Sigma_{\tilde{x},k-1}^+ A_{k-1}^T + \Sigma_w. \end{aligned}$$

Measurement update for the state filter

$$\begin{aligned} L_k^x &= \Sigma_{\tilde{x},k}^- (C_k^x)^T [C_k^x \Sigma_{\tilde{x},k}^- (C_k^x)^T + \Sigma_v]^{-1} \\ \hat{x}_k^+ &= \hat{x}_k^- + L_k^x [y_k - g(\hat{x}_k^-, u_k, \hat{\theta}_k^-)] \\ \Sigma_{\tilde{x},k}^+ &= (I - L_k^x C_k^x)\Sigma_{\tilde{x},k}^-. \end{aligned}$$

Measurement update for the weight filter

$$\begin{aligned} L_k^\theta &= \Sigma_{\tilde{\theta},k}^- (C_k^\theta)^T [C_k^\theta \Sigma_{\tilde{\theta},k}^- (C_k^\theta)^T + \Sigma_e]^{-1} \\ \hat{\theta}_k^+ &= \hat{\theta}_k^- + L_k^\theta [y_k - g(\hat{x}_k^-, u_k, \hat{\theta}_k^-)] \\ \Sigma_{\tilde{\theta},k}^+ &= (I - L_k^\theta C_k^\theta)\Sigma_{\tilde{\theta},k}^-. \end{aligned}$$

# 4. Simplified Dual EKF Methods

The full dual/joint EKF methods are computationally intensive. If precise values for the full set of cell model parameters are not necessary, then other methods might be used. Here, we present methods to determine cell capacity and resistance using EKF-based methods. The change in capacity and resistance from the nominal "new-cell" values give capacity fade and power fade, which are the most commonly employed indicators of cell SOH.

## 4.1 Estimating Resistance

To estimate cell resistance using an EKF mechanism, we formulate a simple model:

$$R_{k+1} = R_k + r_k$$
$$y_k = \mathrm{OCV}(z_k) - i_k R_k + e_k$$

where $R_k$ is the cell resistance and is modeled as a constant value with a fictitious noise process $r_k$ allowing adaptation. $y_k$ is a crude estimate of the cell's voltage, $i_k$ is the cell current, and $e_k$ models estimation error. If we use an estimate of $z_k$ from the state EKF, or from some other source, then we simply apply an EKF to this model to estimate cell resistance. In the standard EKF, we compare the model's prediction of $y_k$ with the true measured cell voltage, and use the difference to adapt $R_k$.

Note that the above model may be extended to handle different values of resistance on charge and discharge, different values of resistance at different SOCs, and different values of resistance at different temperatures, for example. The scalar $R_k$ would be changed into a vector comprising all of the resistance values being modified, and the appropriate element from the vector would be used each time step of the EKF during the calculations.

## 4.2 Estimating Capacity

To estimate cell capacity using an EKF, we again formulate a simple cell model:

$$C_{k+1} = C_k + r_k$$
$$0 = z_k - z_{k-1} + \eta_i i_{k-1} \Delta t / C_{k-1} + e_k.$$

Again, an EKF is formulated using this model to produce a capacity estimate. As the EKF runs, the computation in the second equation (right-hand-side) is compared to zero, and the difference is used to update the capacity estimate. Note that good estimates of the present and previous states-of-charge are required, possibly from an EKF estimating SOC. Estimated capacity may again be a function of temperature (and so forth), if desired, by employing a capacity vector, from which the appropriate element is used in each time step of the EKF during calculations.

# 5. The ESC Cell Model

In order to use these methods, we require an electrical input-output model of the behavior of the electrochemical cells being used; in our case, a Lithium Ion Polymer Battery (LiPB) technology. The cells are treated as nonlinear dynamic systems, represented in a discrete-time state-space form. We assume the form of Equations (1) and (2).

Many cell models have been proposed in the literature for many purposes. The specific application we have in mind is to model cell dynamics for the purpose of state-of-charge estimation in a hybrid electric vehicle (HEV) battery pack. The HEV application is a very harsh environment with rate requirements up to about ±40C, very dynamic rate profiles, and operating temperatures between –30ºC and 50ºC. This is in contrast to relatively benign portable-electronic applications with constant power output and fractional C rates. Methods for cell modeling and SOC estimation that work well in port-

able electronic devices often fail in the HEV application. If precise SOC estimation is required by the HEV, then a very accurate cell model is necessary.

The model that we use in this paper is one that we have called the "enhanced self-correcting" (ESC) cell model [3,5]. In order to use the Kalman methods we propose to estimate SOC, the cell model must be represented in the discrete-time state-space form of (1) and (2) with the constraint that SOC is a member of the state vector. The difference between the models, then, depends only on the definitions of $x_k$, $u_k$, $f(\,)$, and $g(\,)$.

The basis for the SOC state-equation is developed as follows: If $z(t) = \text{SOC}$, we know that

$$z(t) = z(0) - \int_0^t \frac{\eta(i(\tau))\, i(\tau)}{C}\, d\tau, \tag{5}$$

where $C$ is the nominal capacity of the cell, $i(t)$ is the cell current at time $t$, and $\eta(i(t))$ is the Coulombic efficiency of the cell. A discrete-time approximate recurrence may then be written as

$$z_{k+1} = z_k - \frac{\eta(i_k)\, i_k\, \Delta t}{C}, \tag{6}$$

where $\Delta t$ is the sampling period (in hours). Equation (6) is used to include SOC in the state vector of the cell model as it is in state equation format already, with SOC as the state and $i_k$ as the input.

The dynamics of the change of polarization voltage are also captured by a state equation. We add "filter states" with linear dynamics:

$$\left[f_{k+1}\right] = \left[\text{diag}(\alpha)\right]\left[f_k\right] + i_k. \tag{7}$$

The vector $\alpha$ has $N$ filter "poles", with $|\alpha| < 1$ for stability, corresponding to time constants of the polarization voltage dynamics. A value of $N \approx 4$ works well.

A further phenomenon captured by a state equation is that of hysteresis. A cell that has recently undergone a charge event will have a higher rest voltage than one that has undergone a discharge event, even at the same SOC. That is, voltage does not decay to OCV, but to OCV plus/minus a factor based on the hysteresis of the cell. We note that hysteresis is not a phenomenon generally associated with lithium-ion systems, since most applications have been in the light portable electronics area where SOC accuracy is not as critical as in the HEV application and where temperatures are not as extreme. It is, however, very pronounced at low temperatures and can lead to SOC errors as large as ±40% if the estimate is based simply on OCV (even with full cell relaxation), particularly with Mn/graphite-based chemistries. The reason is the spread between the charge and discharge characteristics coupled with the flat nature of the curves between 10% and 90% SOC.

A hysteresis state implementing a linear-time-varying difference equation may be modeled as:

$$h_{k+1} = \exp\left(-\left|\frac{\eta(i_k) i_k \gamma \Delta t}{C}\right|\right) h_k + \left(1 - \exp\left(-\left|\frac{\eta(i_k) i_k \gamma \Delta t}{C}\right|\right)\right) M(z,\dot{z}). \tag{8}$$

$M(z,\dot{z})$ is a static function representing the maximum hysteresis at the present SOC and rate-of-change of SOC, and $\gamma$ is a hysteresis rate constant

The three components of the system state are combined, resulting in

$$x_k = \begin{bmatrix} f_k^T & h_k & z_k \end{bmatrix}^T. \tag{9}$$

The corresponding equations for $f_k$, $h_k$, and $z_k$ then combine to form the vector function $f(\,)$.

The cell terminal voltage is modeled by the output equation $g(\,)$. With the states of the system as defined, the ESC model computes:

$$y_k = \mathrm{OCV}(z_k) + C\left[f_k\right] - Ri_k + h_k. \tag{10}$$

The voltage is computed as the sum of the open-circuit-voltage at the present SOC, plus a weighted sum of the polarization voltage states, minus ohmic losses, plus hysteresis. A further constraint on (10) is that during a constant-current dis/charge, the polarization filter voltages must converge to zero so that $y_k \rightarrow \mathrm{OCV(SOC)} - I \times R$ (plus hysteresis). This constraint is satisfied if the filter has zero dc gain [5], which may be enforced in the filter design.

The form of the ESC model is now completely described. In order to implement the model for a specific cell electrochemistry, however, we require knowledge of the parameters of the model. Specifically, we must determine the OCV versus SOC relationship, the filter time constants $\alpha$, the number of filter states N, hysteresis rate factors, and so forth. In the following sections, we describe how this was done for our prototype cells, and some modeling results.

## 6. Cell Description and Cell Tests for Validation

In this section, we describe cell tests performed to gather cell performance data, and how the data was analyzed to arrive at new-cell numeric values for the parameters of the ESC model. Note that the cells used in this paper differ electrochemically from those reported in previous work [1–6]. We refer to the older cells as GEN3 cells, and to the newer cells as G4 cells. The GEN3 cells are high-power (>20C capable) 7.5Ah Mn spinel/graphite LiPB, and the G4 cells are very high power (>30C capable) 5Ah Mn spinel/blended-carbon LiPB, both reported in [7].

The data comprised tests at –30, –20, –10, 0, 10, 25, 35 and 45 degrees Celsius where sequences of UDDS drive cycles were conducted over the entire SOC range for each test. Cell modeling over an extended temperature range is described in [8]. For simplicity, we consider only the 25ºC test in this paper. The UDDS current versus time profile was generated by NREL's ADVISOR program [9], scaled for a small sedan. Each cycle resulted in a slight elevation of SOC, so the test script executed 15A×1.5 min = 0.375 Ah discharges (13% SOC) between cycles so that the overall testing process would spread over the operational SOC range. If any cycle resulted in a voltage outside of the 2.5V to 4.2V range, that particular cycle was aborted, and the script continued to the subsequent discharge and repeat portion of the sequence. The procedure that we followed was:

1. Soak cell at 25ºC for at least 2 hours.
2. Charge the cell: CC @ 1C (5A) to 4.2V, CV @ 4.2V to 0.01A.
3. Execute the test profile, comprising 22 UDDS cycles separated by discharges and 5 min rests.

Data points were collected periodically, including time, current, voltage, Ah discharged and Ah charged. A representative plot of cell terminal voltage as a function of time is plotted for the room-temperature test in the left frame of Figure 2. In the right frame, a zoomed-in region is shown to magnify detail.

Initial data fitting for an enhanced self-correcting cell model was performed using an optimization procedure and data collected from cells. The model used three filter states, one hysteresis state, and one SOC state, so the set of parameters to be optimized was:

$$\theta = \left[\eta,\ \ C,\ \ \alpha_1 \cdots \alpha_3,\ \ g_1 \cdots g_2,\ \ \gamma,\ \ R,\ \ M\right]^T.$$

Optimization was initialized by providing a preliminary estimate for $\theta$. The ESC model was then run (open-loop) using cell-test current data as input, and the model output voltage was recorded. After an entire data set was simulated by the ESC model for a particular $\theta$, (*i.e.*, all 22 UDDS cycles, dis-

charges and rests), the root-mean-squared (RMS) difference between simulated model output voltage and measured cell output voltage was used as an indicator of the utility of the parameter set $\theta$. The parameters were modified in a direction to reduce RMS error, and the procedure iterated. When RMS error converged, the optimization was terminated. Optimization was done using Matlab's Optimization Toolbox, although any appropriate method might have been used.

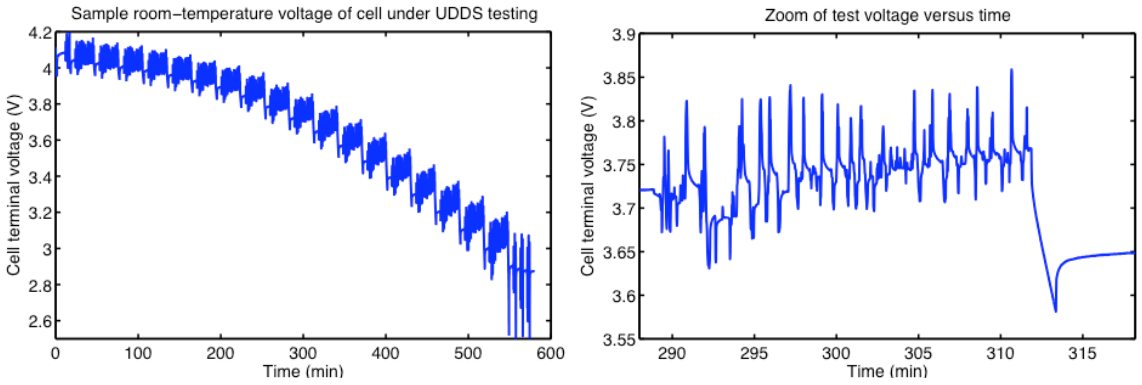


**Figure 2:** Voltage versus time for a representative cell test for dynamic modeling.

## 7. Results of Dual EKF

We have elsewhere shown examples of convergence of state and parameter estimates using GEN3 cells [6]. Here, we focus on dual estimation results for G4 cells (joint estimation gives quite similar results). Representative results are shown in Figure 3. In frame (a), we see that the capacity of the cell does not change appreciably over the period of the cell test of nine hours, but in frame (b) we see that the resistance of the cell changes noticeably. The latter is mostly due to the SOC going from 100% down to about 0% in the cell test, and the fact that the cell's resistance is larger at extreme values of SOC than at intermediate values. The quickly varying nature of the resistance estimates allows slightly better SOC (and other state) estimation using dual/joint EKF than standard EKF since the standard EKF assumes a fixed value of resistance.

If the complexity of the dual EKF is not warranted by an application, the simplified filters from Section 4 may be used. Results using these methods are plotted in frames (c) and (d). In frame (c), the state of the auxiliary capacity estimation filter was initially set about 20% too high and adaptation was allowed to occur. In frame (d) the states of the auxiliary resistance estimation filter were also given erroneous initial values, and adaptation was allowed to occur. In both cases, the estimates converge to the correct values.

The horizontal axis for the plots was determined by noting that a UDDS cycle covers 7.45 miles, and that the UDDS test has 18 such (full) cycles in it. Many repetitions of the UDDS test were required for parameter convergence. Is convergence fast enough? If we consider that the capacity of an HEV cell must degrade less than 20% over a vehicle lifetime (say, 150,000 miles), then the time constant of capacity change is in the order of 50,000 miles. For an estimator to track a moving target, its time constant must be at least four times faster than that of the moving target (faster is better). Here, we see that the capacity filter time constant is in the order of 1000 miles, and the resistance filter time constant is in the order of 500 miles. Both filters are faster than they need be. Note that this example is extreme; in an application the HEV cells would be mass-produced with high quality control and tight tolerances on initial capacity and resistance. The filters would then be initialized with accurate values, and are fast enough to track changes. In fact, the filters can be "tuned" by varying the values for $\Sigma_r$ and $\Sigma_e$ to be either faster or slower than those shown. Faster filters do converge more quickly, but

produce noisier steady-state estimates. Slower filters produce cleaner steady-state estimates. The tuning of the filter must be done to meet design specifications.

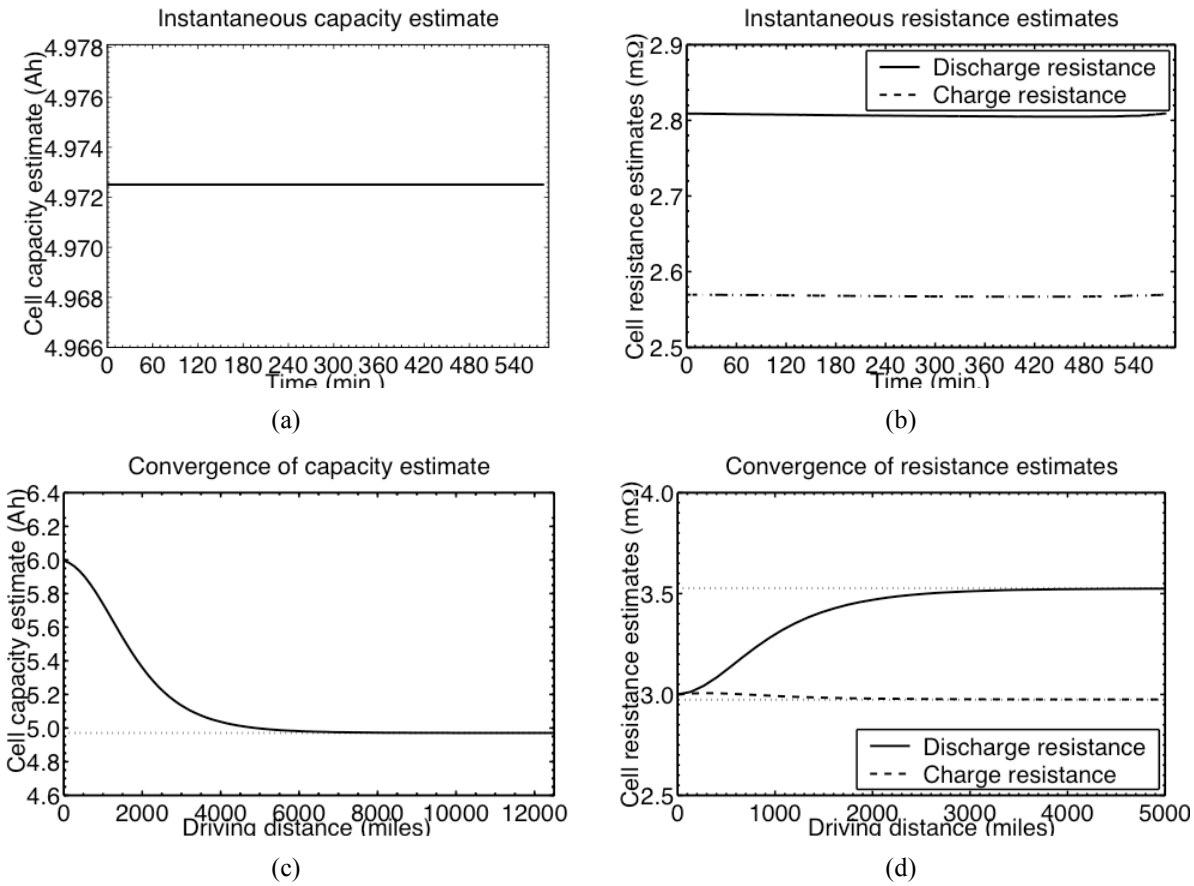


**Figure 3:** Representative results.

# 8. Conclusions

Battery packs that must retain accurate SOC estimation over long terms of deployment require algorithms that can adapt to the aging cell characteristics. We have shown that dual and joint EKF are two possible methods to simultaneously estimate SOC over the lifetime of the pack, as well as accurately estimate parameters. If the complexity of dual/joint EKF is not warranted by an application, then simplified versions may be implemented, as discussed. We have also presented modifications to the standard dual/joint EKF procedure to ensure convergence of the estimated state to the physical state of the battery.

# References


[1] Plett, G., "LiPB dynamic cell models for Kalman-filter SOC estimation," in *CD-ROM Proceedings of the 19th International Battery, Hybrid and Fuel Cell Electric Vehicle Symposium & Exhibition (EVS19)*, Busan, Korea, (October 2002).

[2] Plett, G., "Kalman-Filter SOC Estimation for LiPB HEV Cells," *Proc. 19th International Battery, Hybrid and Fuel Cell Electric Vehicle Symposium & Exhibition (EVS19),* , Busan, Korea, (October 2002).

[3] Plett, G., "Advances in EKF LiPB SOC Estimation," in *CD-ROM Proceedings of the 20th Electric Vehicle Symposium (EVS20),* Long Beach CA, (November 2003).

[4] Plett, G., "Extended Kalman Filtering for Battery Management Systems of LiPB-Based HEV Battery Packs—Part 1: Background," *Journal of Power Sources*, Vol. 134, No. 2, August 2004, pp. 252–61.

[5] Plett, G., "Extended Kalman Filtering for Battery Management Systems of LiPB-Based HEV Battery Packs—Part 2: Modeling and Identification," *Journal of Power Sources*, Vol. 134, No. 2, August 2004, pp. 262–76.

[6] Plett, G., "Extended Kalman Filtering for Battery Management Systems of LiPB-Based HEV Battery Packs—Part 3: State and Parameter Estimation," *Journal of Power Sources*, Vol. 134, No. 2, August 2004, pp. 277–92.

[7] Kim, S.W., Yu, J.S. Namgoong, J. Kim, J.H., Kim, M.H., "Progress in Li-ion Polymer Battery and Pack System of LG Chem. For Transportation Applications," in *CD-ROM Proceedings of the 20th Electric Vehicle Symposium (EVS20),* Long Beach CA, (November 2003).

[8] Plett, G., "Results of Temperature-Dependent LiPB Cell Modeling for HEV SOC Estimation," *Proc. 21st International Battery, Hybrid and Fuel Cell Electric Vehicle Symposium & Exhibition (EVS21),* Monaco, (April 2005).

[9] CTTS Vehicle Systems Analysis Homepage, http://www.ctts.nrel.gov/analysis/, accessed May 2003.

[10] S. Haykin (Ed.), *Kalman Filtering and Neural Networks*, (Wiley Inter-Science: New York), 2001.

# Author

**Dr. Gregory L. Plett,** *Assistant Professor,*
Dept. of Electrical and Computer Engineering, University of Colorado at Colorado Springs,
1420 Austin Bluffs Parkway, P.O. Box 7150, Colorado Springs, CO 80933–7150 USA
Tel: +1–719–262–3468, Fax: +1–719–262–3589, E-mail: glp@eas.uccs.edu,
URL: http://mocha-java.uccs.edu, *and consultant to*
Compact Power Inc., 1200 S. Synthes Ave., Monument, CO 80132 USA
Tel: +1–719–488–1600x134, Fax: +1–719–487–9485, E-mail: gplett@compactpower.com.
URL: http://www.compactpower.com/.